*Journal of Advanced Ceramics*
2016, **5**(3): 197–203
DOI: 10.1007/s40145-016-0190-4

ISSN 2226-4108
CN 10-1154/TQ

**Research Article**

# Synthesis of ferromagnetic $La_{1-x}Sr_xMnO_3$ nanoparticles by precipitation from diethylene glycol solution and their properties

Yulia SHLAPA[a,*], Sergii SOLOPAN[a], Oleksandr YELENICH[a], Volodymyr TRACHEVSKII[b], Anatolii BELOUS[a]

[a] *V.I. Vernadsky Institute of General and Inorganic Chemistry, NAS of Ukraine, 32/34 Palladina Avenue, 03680, Kyiv 142, Ukraine*
[b] *Technical Center NAS of Ukraine*

Received: November 30, 2015; Revised: April 12, 2016; Accepted: April 25, 2016


**Abstract:** $La_{1-x}Sr_xMnO_3$ nanoparticles were synthesized by precipitation from diethylene glycol solution. Features of synthesis were studied using $^{1}H$, $^{13}C$, $^{139}La$ nuclear magnetic resonance (NMR) investigations. The obtained results showed that the complexation reaction between diethylene glycol and metal cations takes place during the synthesis. These complexes decomposed at 200 ℃ and an amorphous precursor (La,Sr)$MnO_3$ was formed. According to X-ray results, the crystallization of the perovskite structure began at 600 ℃ and finished at 800 ℃. Microstructural studies showed that obtained nanoparticles are weakly agglomerated and have small sizes. Based on these nanoparticles, magnetic fluid was prepared which was effectively heated under an alternating magnetic field.

**Keywords:** manganite; perovskite; precipitation; complexation reaction; diethylene glycol; nuclear magnetic resonance (NMR)

## 1 Introduction

At present, ferromagnetic materials find numerous practical applications in different fields of science and engineering and, particularly, in medicine [1]. Drug delivery, therapy, and diagnostic (magnetic resonance imaging, MRI) can be possible directions of medical usage of ferromagnetic nanoparticles [2,3]. It is connected with the fact that there is some information about compatibility of several ferromagnetic materials (magnetite—$Fe_3O_4$) with biological objects [4]. Moreover, application of magnetic nanoparticles in medicine allows improving medical treatment techniques [5]. For instance, using them for MRI permits increasing the image contrast [6]. The application of magnetic nanomaterials in drug delivery gives an opportunity to decrease the dosage of injected medicine [7], drug injection becomes local, and thus negative influence of toxic compounds on healthy tissues can be avoided [8]. It also should be mentioned that we could improve hyperthermia treatment of malignant tumors by using magnetic nanoparticles [9]. Hyperthermia has a number of problems to be solved. For example, this method does not allow heating deep-seated tumors [10]. To tackle them, scientists offer to use ferromagnetic magnetite ($Fe_3O_4$) nanoparticles [11]. This material has many advantages: we can obtain it in the crystalline form at comparatively low temperatures, nanoparticles have necessary sizes for medical treatment and they are weakly agglomerated, and they have already been used in medicine (for MRI)

* Corresponding author.
E-mail: yuliashlapa@ukr.net

[12]. However, magnetite has an essential drawback as it has a high Curie point (585 ℃) that causes uncontrolled heating to high temperatures. Consequently, it results in destroying healthy tissues.

Therefore, heterosubstituted lanthanum manganites $La_{1-x}Sr_xMnO_3$ ($x = 0.2$–$0.4$) with the distorted perovskite structure and ferromagnetic properties are of particular interest due to their Curie temperature that can be changed in the range of 20–70 ℃ [13]. It could allow heating tumors to certain temperatures, particularly, to the Curie temperature.

As it is known, nanoparticles for medical application must be nanosized, single-domain, weakly agglomerated, and nontoxic. In addition, there should not be any interactions between individual nanoparticles, i.e., they must be superparamagnetic [14]. Such nanoparticles must be effectively heated in an alternating magnetic field (to temperatures 42–45 ℃) for a possible application in hyperthermia treatment. That is, they must demonstrate high specific loss power (SLP) values.

Among well-known synthesis methods of nanoparticles of heterosubstituted lanthanum manganites, we can single out sol–gel method [15–17], co-precipitation from aqueous solutions [18], synthesis by precipitation from microemulsions [19], which allow obtaining nanoparticles in a wide range of size and property. However, each of the above-mentioned methods has drawbacks. For instance, there are many so-called "bridge" bonds between individual nanoparticles during the synthesis by sol–gel method and these particles are strongly agglomerated after heat treatment. When nanoparticles are synthesized by precipitation from aqueous solutions and microemulsions (where metal nitrates are used as raw reagents and CTAB (cetyl trimethylammonium bromide) in hexanol environment as a surfactant), crystallization of single-phase product takes place at temperatures higher than 1000 ℃. This is due to the formation of stable intermediate phases and it causes significant growth and agglomeration of particles.

The synthesis by precipitation from diethylene glycol solution can be one of the possible ways of obtaining nanoparticles with necessary properties. Previously, this technique allowed obtaining weakly agglomerated ferrite nanoparticles with spinel structure [20]. However, there is no information about synthesis of manganite nanoparticles by precipitation from diethylene glycol solution.

The aim of this study was to investigate the features of synthesis of nanoparticles based on substituted lanthanum–strontium manganites $La_{1-x}Sr_xMnO_3$ from diethylene glycol solution, and their structure and physical properties.

## 2 Materials and methods

Ferromagnetic lanthanum–strontium manganite $La_{1-x}Sr_xMnO_3$ nanoparticles with perovskite structure were synthesized by precipitation from diethylene glycol solution according to the scheme shown in Fig. 1.

Concentrated aqueous solutions of metal salts $Mn(NO_3)_2$ ($C_m = 3$ mol/L), $La(NO_3)_3$ ($C_m = 1.3$ mol/L), $Sr(NO_3)_2$ ($C_m = 0.2$ mol/L) were used as starting materials. Sodium hydroxide (NaOH) was used for precipitation of metal hydroxides. Diethylene glycol (DEG) was used as a reaction medium and oleic acid (OLA) as a stabilizer.

To obtain nanoparticles of heterosubstituted $La_{1-x}Sr_xMnO_3$ ($x = 0.225$) manganite, necessary molar amounts of metal salt solutions $La(NO_3)_3$, $Sr(NO_3)_2$, $Mn(NO_3)_2$ were added to diethylene glycol in a three-neck flask. Solution of NaOH in DEG was prepared separately. Solution of sodium hydroxide in diethylene glycol was added to the salt mixture in a dropwise manner when stirring. The obtained reaction mixture was stirred for 1 h, heated on the oil bath with the heating rate of 2–3 ℃/min to 200 ℃, and kept for 1 h. The formation of the precipitate was observed during the heating of the reaction mixture. Oleic acid solution

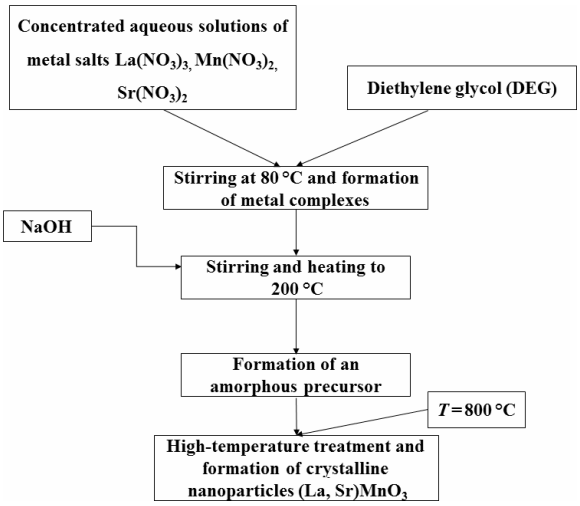


**Fig. 1** General scheme of synthesis of $La_{1-x}Sr_xMnO_3$ nanoparticles from diethylene glycol solution.

was added to the system after heat treatment, stirred, and left to be cooled to room temperature. Particles were separated by centrifugation with the rate of 5000 turn/min and dispersed in ethyl alcohol. The obtained powder was dried in air at 30–50 ℃. The freshly deposited particles were subjected to the heat treatment in air at different temperatures for 2 h.

Chemical reactions taking place during the synthesis of $La_{1-x}Sr_xMnO_3$ nanoparticles from diethylene glycol solution were monitored by $^{1}H$, $^{13}C$, $^{139}La$ nuclear magnetic resonance (NMR) studies on the AVANCE 400 (Bruker) spectrometer in the temperature range of 25–50 ℃.

X-ray investigations were performed on the DRON 4-07 diffractometer (Cu Kα radiation). Lattice parameters of the single-phase product were calculated by the Rietveld method using FULL-PROF software package [21].

The particle size and morphology were analyzed by transmission electron microscope (TEM) JEOL JEM-1230. The particle size distribution was calculated from TEM images as described in Ref. [22] and using Image Tool 3 and OriginPro 8.5 SR1software packages.

The measurements of SLP for magnetic fluid based on synthesized nanoparticles and aqueous agarose solution were done according to Ref. [23] in the alternating magnetic field (frequency of 300 kHz, amplitude of 9.6 kA/m). SLP values were calculated by Eq. (1):

$$\mathrm{SLP} = \frac{C_{\mathrm{fluid}} \cdot V_{\mathrm{s}}}{m_{\mathrm{powder}}} \cdot \frac{\mathrm{d}T}{\mathrm{d}\tau} \tag{1}$$

where $\mathrm{d}T/\mathrm{d}\tau$ is the initial slope of the temperature versus time curve, $C_{\mathrm{fluid}}$ is the specific heat of the solvent, $V_{\mathrm{s}}$ is the sample volume, and $m_{\mathrm{powder}}$ is an amount of magneto-active material in magnetic fluid.

## 3 Results and discussion

### 3. 1 NMR investigations

Figures 2 and 3 show the $^{1}H$ and $^{13}C$ NMR spectra of metal salt solutions in diethylene glycol, respectively, and signal parameters are given in Table 1.

There are four signals in $^{1}H$ NMR spectrum of diethylene glycol (DEG). In accordance with Ref. [24], they belong to four types of unequal protons: water protons (A) and –OH groups (B), $–CH_2–OH$ (C) and $–CH_2–O–$ (D) ($\delta$ values of appropriate signals are given in Table 1). Signals C and D of free diethylene glycol molecules are supposed to be triplets by spin–spin interaction of protons of neighbor $–CH_2–$ groups [25]. However, as the measurements have shown, they represent a superposition of several groups of hyperfine interaction components. It indicates that there are

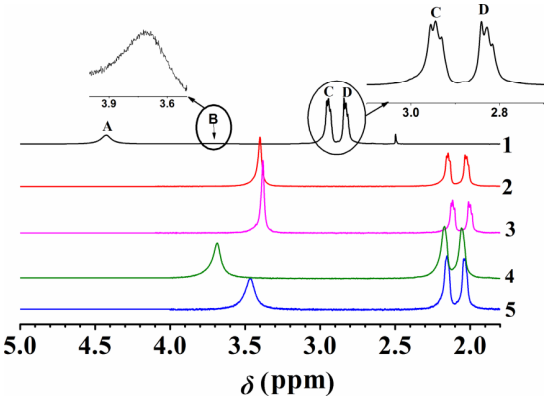


**Fig. 2** $^{1}H$ NMR spectra: 1—DEG; 2—DEG + $Sr(NO_3)_2$; 3—DEG + $Sr(NO_3)_2$ + NaOH; 4—DEG + $La(NO_3)_3$; 5—DEG + $La(NO_3)_3$ + NaOH.

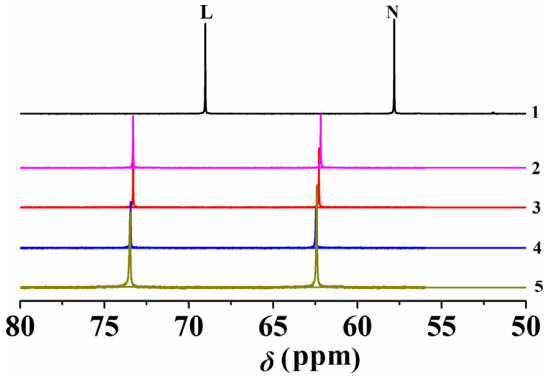


**Fig. 3** $^{13}C$ NMR spectra: 1—DEG; 2—DEG + $Sr(NO_3)_2$; 3—DEG + $Sr(NO_3)_2$ + NaOH; 4—DEG + $La(NO_3)_3$; 5—DEG + $La(NO_3)_3$ + NaOH.

**Table 1 Signal parameters of $^{1}H$, $^{13}C$ NMR spectra of metal salt solutions in diethylene glycol**

| | Chemical shift $^{1}H$ (ppm) | | | | Chemical shift $^{13}C$ (ppm) | |
|---|---|---|---|---|---|---|
| | A | B | C | D | L | N |
| | $H_2O$ | –OH | $–CH_2–OH$ | $–CH_2–O–$ | $–CH_2–OH$ | $–CH_2–O–$ |
| DEG | 4.420 | 3.710 | 2.950 | 2.820 | 69.000 | 57.820 |
| DEG + $Sr(NO_3)_2$ | 3.400 | — | 2.147 | 2.022 | 73.301 | 62.286 |
| DEG + $Sr(NO_3)_2$ + NaOH | 3.381 | — | 2.116 | 1.999 | 73.305 | 62.182 |
| DEG + $La(NO_3)_3$ | 3.685 | — | 2.171 | 2.052 | 73.454 | 62.472 |
| DEG + $La(NO_3)_3$ + NaOH | 3.467 | — | 2.153 | 2.035 | 73.490 | 62.413 |

associates in which molecules are in different conformational states (Fig. 2 (spectrum 1)).

Two signals of unequal groups (finite and internally chain) $–CH_2–OH$ (L) and $–CH_2–O–$ (N) are in $^{13}C$ NMR spectrum of diethylene glycol (Fig. 3 (spectrum 1)).

Figures 2 (spectrum 2) and 3 (spectrum 2) show the $^1H$ and $^{13}C$ NMR spectra of $Sr(NO_3)_2$ solution in diethylene glycol, respectively. According to Ref. [26], diethylene glycol (as a representative of polyhydric alcohols) can react with metal hydroxides, forming alkoholates. There are three signals in $^1H$ NMR spectrum of $Sr(NO_3)_2$ solution in diethylene glycol (Fig. 2 (spectrum 2)), which belong to three types of unequal protons A, C, and D. The absence of signal B in the spectrum, that is typical of alcohol –OH group, confirms the complexation reaction between diethylene glycol and $Sr^{2+}$ cations in alkaline medium according to Scheme (2) (simplistic view). The shift of signals A, C, and D to the strong field (Fig. 2) can be explained by the fact that the complexation between diethylene glycol and $Sr^{2+}$ cation causes an increase in screening of protons of ligand functional groups in binding with strontium atom.

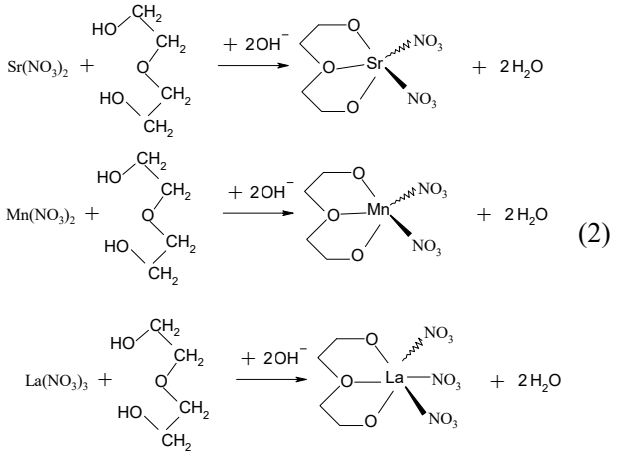


(2)

The change of signals in $^1H$, $^{13}C$ NMR spectra of $La(NO_3)_3$ solution in diethylene glycol (Fig. 2 (spectrum 4) and Fig. 3 (spectrum 4)) owing to the complexation reaction can be explained in the same way. The same reactions take place between diethylene glycol molecules and $Mn^{2+}$ ions. However, it is impossible to obtain informative NMR spectra because of ferromagnetic properties of manganese.

The displacements of the different signals remain quasiunchanged with the addition of hydroxyl groups (Table 1). It shows that the strontium–diethylene glycol complex structure does not change very much after reacting with hydroxyl groups. There is a replacement of both external and internal spheres of the complexing ion compared to corresponding lanthanum complex: nitrate groups are replaced by hydroxyl groups, and hydroxocomplex with $Na^+$ ions in the outer sphere is formed. Increase in chemical shift values for signals L and N is observed in $^{13}C$ NMR spectra (Fig. 3). On this basis, the evolution of coordination sphere of metal ions under the action of alkali can be represented by Scheme (3).

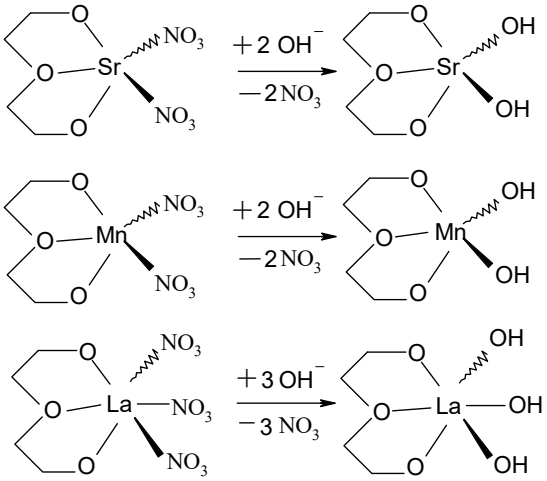


(3)

The addition of sodium hydroxide to the La $(NO_3)_3$–diethylene glycol system causes the same interaction, forming hydroxocomplexes (Fig. 2 (spectrum 5) and Fig. 3 (spectrum 5)). There are some reasons to consider that similar transformations take place in the system with $Mn^{2+}$.

There are three signals F, E, and K in $^{139}La$ NMR spectrum of $La(NO_3)_3$–diethylene glycol system (Fig. 4 (spectrum 2)) with corresponding values of chemical shifts (Table 2). It indicates that there are unequal $La^{3+}$ forms in the reaction medium. Oxygen of diethylene glycol OH groups causes the displacement of $^{139}La$ signal towards the weak field, and oxygen of $–CH_2–O–CH_2–$ groups displaces the signal towards the strong field. The signal at –640.0 ppm belongs to $La^{3+}$ ion for which nitrate ion is a ligand in the coordination sphere. Transition of the nitrate complex into the hydroxo form can be observed when adding the alkali (NaOH) into the investigated system. The shift of the signals in the spectrum (Fig. 4 (spectrum 3)) is quasiunchanged when adding OH groups.

The signal (Q) appears in the spectrum of $La(NO_3)_3$–DEG system (Fig. 4 (spectra 4 and 5)) after adding strontium nitrate. This signal can be identified as a signal of free $La^{3+}$ ions. Their appearance is caused by

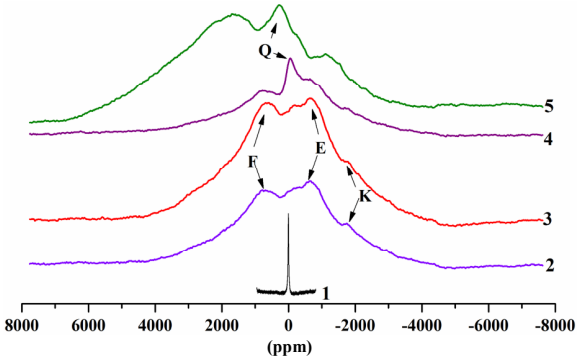


**Fig. 4** $^{139}$La NMR spectra: 1—La; 2—DEG + $La(NO_3)_3$; 3—DEG + $La(NO_3)_3$ + NaOH; 4—DEG + $La(NO_3)_3$ + $Sr(NO_3)_2$; 5—DEG + $La(NO_3)_3$ + $Sr(NO_3)_2$ + NaOH.

**Table 2 Signal parameters of $^{139}$La NMR spectra**

| No. | | Chemical shift $^{139}$La (ppm) | | | |
|---|---|---|---|---|---|
| | | F | E | K | Q |
| 1 | $La(NO_3)_3$ | — | — | — | — |
| 2 | DEG + $La(NO_3)_3$ | 729.6 | –640.8 | –1766.3 | — |
| 3 | DEG + $La(NO_3)_3$ + NaOH | 729.6 | –640.0 | –1766.3 | — |
| 4 | DEG + $La(NO_3)_3$ + $Sr(NO_3)_2$ | 729.6 | –140.8 | –1766.3 | –64 |
| 5 | DEG + $La(NO_3)_3$ + $Sr(NO_3)_2$ + NaOH | 1983.9 | –140.8 | –1254.4 | 307.2 |

the competitive complexation of $La^{3+}$ and $Sr^{2+}$ ions due to which the $Sr^{2+}$ ion displaces the $La^{3+}$ ion from the coordination environment. The injection of NaOH into the reaction mixture leads to the shift of signals towards the weak field, and it confirms the substitution of nitrate ions for hydroxyl ions in the coordination sphere of the complex.

An amorphous precursor of co-precipitated nanoparticles is formed after heating hydroxocomplexes in the reaction medium to 200 ℃ according to Scheme (4):

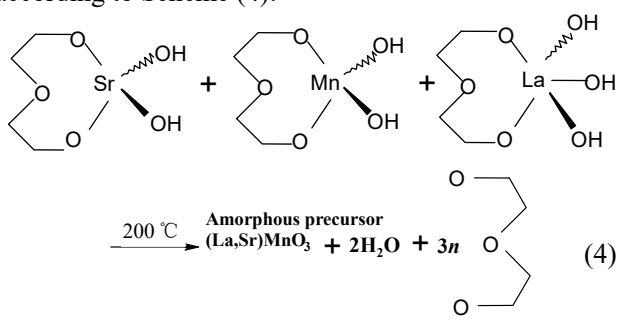


(4)

## 3. 2 X-ray studies

X-ray data for $La_{1-x}Sr_xMnO_3$ manganite samples annealed at different temperatures are shown in Fig. 5. The obtained results show that an amorphous phase is formed at the synthesis temperature, and the crystallization of the perovskite structure begins at 600 ℃ and completely finishes at 800 ℃.

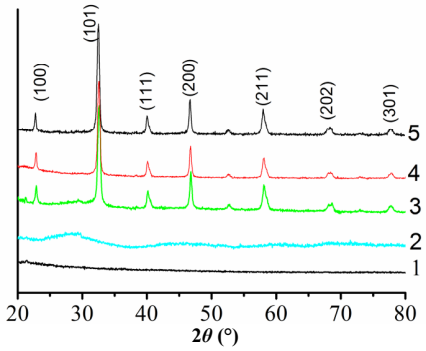


**Fig. 5** X-ray data for $La_{1-x}Sr_xMnO_3$ powder synthesized from diethylene glycol solution at: 1—200 ℃; 2—500 ℃; 3—600 ℃; 4—700 ℃; 5—800 ℃.

Crystallographic parameters of manganite nanoparticles obtained after the heat treatment at 800 ℃ are $a$ = 5.4992(3) Å, $c$ = 13.358(1) Å, and $V$ = 349.85(4) Å$^3$ (Bragg factor $R_B$ = 7.39%, compliance form factor $R_f$ = 6.10%). An average crystalline particle size of $La_{0.775}Sr_{0.225}MnO_3$ nanoparticles was calculated from the obtained X-ray patterns by Scherrer's equation and it is approximately 22 nm.

## 3. 3 TEM investigations of the particle morphology

To study the morphology of synthesized nanoparticles and calculate their size, microstructural investigations were done. They were compared to nanoparticles synthesized by sol–gel method [15] (Fig. 6). The obtained results show that nanoparticles precipitated from diethylene glycol solution are weakly agglomerated and they have the particle size distribution in the range of 15–45 nm. When

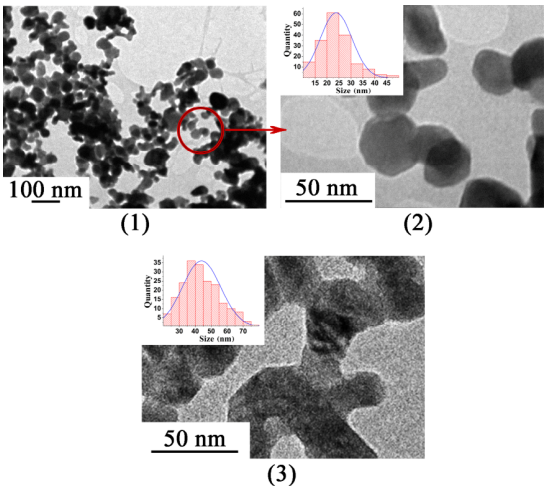


**Fig. 6** TEM images for $La_{1-x}Sr_xMnO_3$ nanoparticles: 1, 2—synthesized by precipitation from non-aqueous diethylene glycol solution and annealing at 800 ℃ for 2 h; 3—synthesized by sol–gel method [15].

$La_{1-x}Sr_xMnO_3$ nanoparticles obtained by precipitation from diethylene glycol solution are weakly agglomerated and have small sizes (Fig. 6(2)), particles obtained by sol–gel method [15,27] agglomerate due to the formation of the so-called "bridges" between individual nanoparticles.

### 3. 4 Measurements of the heating efficiency

Magnetic fluid based on the obtained $La_{1-x}Sr_xMnO_3$ nanoparticles and aqueous agarose solution was developed as described in Ref. [23]. This magnetic fluid was effectively heated under the alternating magnetic field. The obtained results of the study of heating temperature versus time under the action of magnetic field are shown in Fig. 7. The value of specific loss power (SLP) was calculated on the basis of these results and it is 14.7 W/g. After comparing $La_{1-x}Sr_xMnO_3$ nanoparticles synthesized by precipitation from diethylene glycol solution with nanoparticles obtained by sol–gel method [15,27], it should be mentioned that there are no "bridge" bonds between individual particles, i.e., they are weakly agglomerated (Fig. 6(2)). Besides, these nanoparticles have smaller sizes. They are effectively heated under the alternating magnetic field. It is quantitatively determined by SLP value. Therefore, nanoparticles and magnetic fluids based on them can be used as inductors for hyperthermia treatment.

## 4 Conclusions

$La_{1-x}Sr_xMnO_3$ manganites with distorted perovskite structure were synthesized by precipitation from diethylene glycol solution. To investigate the chemical reactions which take place during the synthesis of $La_{1-x}Sr_xMnO_3$ nanoparticles, $^{1}H$, $^{13}C$, $^{139}La$ NMR studies were done. According to the obtained results, after the chemical interaction, monometallic complexes between metals and diethylene glycol are formed and metal ions are influenced by oxygen atoms of diethylene glycol functional groups in these complexes. Adding sodium hydroxide (NaOH) to the complexes leads to their transition into hydroxocomplexes. They decompose forming an amorphous precursor $(La,Sr)MnO_3$ after heating to 200 ℃. Crystalline perovskite structure is formed after further heating at 800 ℃. The results of microstructural studies showed that the obtained nanoparticles are weakly agglomerated and have a narrow particle size distribution. SLP value for these nanoparticles is 14.7 W/g. It enables to use them as the inductors of hyperthermia treatment.

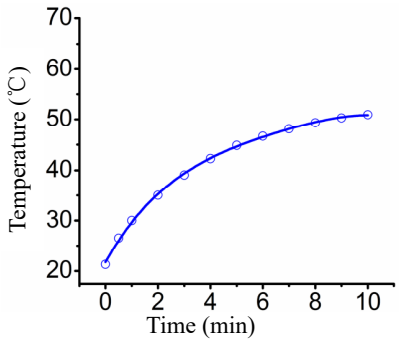


**Fig. 7** Dependence of heating temperature versus time for magnetic fluid based on $La_{1-x}Sr_xMnO_3$ nanoparticles obtained by precipitation from diethylene glycol solution.

## References

[1] Pankhurst QA, Connolly J, Jones SK, *et al*. Applications of magnetic nanoparticles in biomedicine. *J Phys D: Appl Phys* 2003, **36**: R167.

[2] Hofmann-Amtenbrink M, von Rechenberg B, Hofmann H. Superparamagnetic nanoparticles for biomedical application. *Nanostructured Materials for Biomedical Applications* 2009, **100**: 119–149.

[3] Veverka P, Kaman O, Kačenka M, *et al*. Magnetic $La_{1-x}Sr_xMnO_3$ nanoparticles as contrast agents for MRI: The parameters affecting $^{1}H$ transverse relaxation. *J Nanopart Res* 2015, **17**: 33.

[4] Ankamwar B, Lai TC, Huang JH, *et al.* Biocompatibility of $Fe_3O_4$ nanoparticles evaluated by *in vitro* cytotoxicity assays using normal, glia and breast cancer cells. *Nanotechnology* 2010, **21**: 075102.

[5] Mornet S, Vasseur S, Grasset F, *et al*. Magnetic nanoparticle design for medical diagnosis and therapy. *J Mater Chem* 2004, **14**: 2161–2175.

[6] Stephen ZR, Kievit FM, Zhang M. Magnetite nanoparticles for medical MR imaging. *Mater Today* 2011, **14**: 330–338.

[7] Arruebo M, Fernández-Pacheco R, Ricardo Ibarra M, *et al*. Magnetic nanoparticles for drug delivery. *Nanotoday* 2007, **2**: 22–32.

[8] Gubin SP, Koksharov YA, Khomutov GB, *et al*. Magnetic nanoparticles: Preparation, structure and properties. *Russ Chem Rev* 2005, **74**: 489–520.

[9] Thiesen B, Jordan A. Clinical applications of magnetic nanoparticles for hyperthermia. *Int J Hyperther* 2008, **24**: 467–474.

[10] Jordan A, Scholz R, Wust P, *et al*. Magnetic fluid hyperthermia (MFH): Cancer treatment with AC magnetic field induced excitation of biocompatible superparamagnetic nanoparticles. *J Magn Magn Mater* 1999, **201**: 413–419.

[11] Jeyadevan B. Present status and prospects of magnetite nanoparticles-based hyperthermia. *J Ceram Soc Jpn* 2010, **118**: 391–401.
[12] Šafařík I, Horská K, Šafaříková M. Magnetic nanoparticles for biomedicine. In *Intracellular Delivery*. Prokop A, Ed. Springer Netherlands, 2011: 363–372.
[13] Vasseur S, Duguet E, Portier J, *et al.* Lanthanum manganese perovskite nanoparticles as possible *in vivo* mediators for magnetic hyperthermia. *J Magn Magn Mater* 2006, **302**: 315–320.
[14] Solopan S, Belous A, Yelenich A, *et al.* Nanohyperthermia of malignant tumors. I. Lanthanum–strontium manganite magnetic fluid as potential inducer of tumor hyperthermia. *Exp Oncol* 2011, **33**: 130–135.
[15] Solopan SO, V'yunov OI, Belous AG, *et al.* Effect of nanoparticles agglomeration on electrical properties of $La_{1-x}A_xMnO_3$ (A = Sr, Ba) nanopowder and ceramic solid solutions. *Solid State Sci* 2012, **14**: 501–505.
[16] Bubnovskaya L, Belous A, Solopan A, *et al.* Nanohyperthermia of malignant tumors. II. *In vivo* tumor heating with manganese perovskite nanoparticles. *Exp Oncol* 2012, **4**: 336–339.
[17] Thorat ND, Otari SV, Bohara RA, *et al.* Structured superparamagnetic nanoparticles for high performance mediator of magnetic fluid hyperthermia: Synthesis, colloidal stability and biocompatibility evaluation. *Mat Sci Eng C* 2014, **42**: 637–646.
[18] Belous AG, Pashkova YV, Vunov OI, *et al.* Effect of processing conditions on the phase transformations, structure and magnetoresistive properties of $La_{0.7}Sr_{0.3}MnO_{3\pm\gamma}$ manganites. *Ukrainian Chemistry Journal* 2005, **71**: 17–23.
[19] Uskoković V, Drofenik M. Synthesis of lanthanum–strontium manganites by oxalate-precursor co-precipitation methods in solution and in reverse micellar microemulsion. *J Magn Magn Mater* 2006, **303**: 214–220.
[20] Yelenich OV, Solopan SO, Trachevskii VV, *et al.* Synthesis and properties of $AFe_2O_4$ (A = Mn, Fe, Co, Ni, Zn) nanoparticles produced by deposition from diethylene glycol solution. *Russ J Inorg Chem+* 2013, **58**: 901–905.
[21] Monshi A, Reza Foroughi M, Reza Monshi M. Modified Scherrer equation to estimate more accurately nano-crystallite size using XRD. *World Journal of Nano Science and Engineering* 2012, **2**: 154–160.
[22] Peddis D, Orrù F, Ardu A, *et al.* Interparticle interactions and magnetic anisotropy in cobalt ferrite nanoparticles: Influence of molecular coating. *Chem Mater* 2012, **24**: 1062−1071.
[23] Veverka M, Závěta K, Kaman O, *et al.* Magnetic heating by silica-coated Co–Zn ferrite particles. *J Phys D: Appl Phys* 2014, **47**: 065503.
[24] Günter H. *NMR Spectroscopy: An Introduction*. New York: Wiley, 1980.
[25] Drago RS. *Physical Methods in Chemistry*, 2nd edn. Philadelphia, PA, USA: Saunders, 1992.
[26] Clayden J, Geeves N, Warren S. *Organic Chemistry*, 2nd edn. Oxford University Press, 2012.
[27] Pollert E, Kaman O, Veverka P, *et al*. Core–shell $La_{1-x}Sr_xMnO_3$ nanoparticles as colloidal mediators for magnetic fluid hyperthermia. *Phil Trans R Soc A* 2010, **368**: 4389–4405.